

## COUPLING MAXWELL'S EQUATION TIME-DOMAIN SOLUTION WITH MONTE-CARLO TECHNIQUE TO SIMULATE ULTRAFAST OPTICALLY CONTROLLED SWITCHES

K.M. Connolly, S.M. El-Ghazaly, R.O. Grondin, and R.P. Joshi\*

Center for Solid State Electronics Research, Arizona State University, Tempe, Arizona 85287-6202

\*Department of Electrical Engineering, Old Dominion University, Norfolk, Virginia 23529-0246

### ABSTRACT

In this paper, we discuss how a combination of direct finite-difference time domain solutions of Maxwell's equations and Monte-Carlo models of photocarrier transport can be used to eliminate assumptions commonly made in developing equivalent circuit models for transmission lines. We then apply this technique to an electro-optic switch with sub-picosecond risetimes.

### INTRODUCTION

To accurately simulate semiconductor devices in the sub-millimeter and upper millimeter wave range, high frequency effects must be included. These effects must be considered when developing switching, small-signal, and large signal models. In large signal and switching problems, there may be large AC fields whose effect upon carrier transport must be considered. This may be accomplished by using the electromagnetic fields obtained by solving Maxwell's equations.

Maxwell's equations however, do not provide a complete mathematical description of the problem. Instead, they must be supplemented by a set of constitutive relations. The problem considered here involves modeling the interaction between electromagnetic waves and free carriers. The carriers appear in Maxwell's equations as sources of electromagnetic fields, and electromagnetic fields appear in the constitutive carrier transport model as forcing functions. A model of the interaction between these two systems can be accurate for high frequencies only if the models of both systems are accurate for subpicosecond time intervals.

We have developed a technique to solve this problem which merges a three dimensional Ensemble Monte-Carlo (EMC) program with a three dimensional solution of Maxwell's equations in the time domain. The time domain was chosen over the frequency domain since the photocarrier transport process is highly nonlinear. Fortunately, we are only interested in time periods on the order of a few picoseconds, thus a direct time-domain solution of Maxwell's equations in conjunction with a Monte-Carlo transport model is possible.

The solution was developed by using a finite difference scheme over a three dimensional mesh covering the entire device. This scheme allows us to obtain the electromagnetic wave propagation and temporal evolution of the electron and

hole distributions throughout the device at every timepoint of the simulation. We have applied this technique in a study of the response of an electro-optic switch consisting of a gap in a microstrip fabricated on semi-insulating GaAs with a LiTaO<sub>3</sub> superstrate.

### THEORY

In the past, photoconductive switches have been modeled as switches inserted between two ideal, lossless transmission lines. While more complicated models have incorporated transmission lines with frequency dependent characteristic impedances, these models are not suited for the present case. Instead, direct solutions of Maxwell's equations are needed for a more general and exact approach. The solution can be outlined in three steps:

#### I. The Electromagnetic Model: Three-Dimensional Finite-Difference Solution of Maxwell's Equations in the Time Domain

Since this technique is developed to study transient conditions inside semiconductors, it must be approached as an initial value problem. An initial, self-consistent distribution of the fields and charges must be specified. If the device is not biased and contains no free charges, it may be assumed that the initial fields are zero. However, when the device is biased, one should initially solve for the DC charges and currents which are the sources of the electric and magnetic fields. The fields may then be obtained from their sources by using a suitable set of equations.

The time domain finite-difference scheme then proceeds to solve the problem in a leapfrog manner. This means that the electric field components are calculated at time  $t$ , followed by the calculation of the magnetic field components at time  $t+\Delta t/2$ . This process is possible since the electric field space and time mesh have been displaced by a half mesh from the magnetic field space and time mesh. This leapfrog solution is continued until the simulation is complete [1].

In real space, these equations must be solved according to appropriate boundary conditions. This means that the tangential electric and magnetic fields must be specified on the device's boundaries. In most cases, the device is surrounded by either metallic surfaces, or open space (i.e. air). The metallic conductors are approximated as perfect conductors, leading to zero tangential electric fields and perpendicular magnetic fields. For open space boundaries, it is not possible

to discretize all space due to computers' limited memory. Therefore, one must simulate open space through the use of absorbing boundary conditions. Absorbing boundary conditions allow outgoing waves to pass through boundaries without reflection. To simulate this one must truncate the finite difference mesh with a plane containing the tangential electric fields and perpendicular magnetic fields. The absorbing boundary condition formulas are then applied to the tangential electric field components. Once the tangential electric field components are known, the perpendicular magnetic field components can be calculated through the use of the normal finite difference equations [2].

## II. The semiconductor model : Ensemble Monte-Carlo Technique

In an EMC simulation, one keeps track of several thousand representative particles by following their trajectories through the system. The particles accelerated by fields, and various individual scattering mechanisms are statistically simulated in order to model energy flow.

EMC is capable of accurately simulating carrier transport in semiconductors on a femto-second scale. In our simulation we use a bipolar EMC based on a three valley electron and a three band hole model for the GaAs substrate with all relevant carrier-phonon and carrier-carrier scattering mechanisms included. The electrodynamic forces influencing the bipolar plasma are considered through a complete model of Lorentz forces, which includes the time evolving electric and magnetic fields. These fields depend upon the local charge imbalance, and are self-consistently calculated in each time step by the the electromagnetic model [3-4].

## III. Coupling the two models

EMC models the response of individual particles to external driving forces. On the other hand, the electromagnetic fields obtained from Maxwell's equations are based on a fluid model. This means that the current generated by individual particles is not observed; only global results are obtained. Thus the link between the two models must be established by properly transforming the physical parameters (e.g. electric field, magnetic field, current density) from one model to the other. This is accomplished by dividing the semiconductor's volume of interest into cubic cells of uniform electric and magnetic fields. These fields are obtained by properly averaging the fields calculated by the electromagnetic model to account for the differences in spatial and temporal mesh definitions. EMC is used inside each cell to calculate carrier velocity and position, and also to trace the carriers crossing the borders of each cell. It is this current density that represents the feedback from the EMC model for updating the electromagnetic fields. Mathematically, it is obtained by adding the contribution of the individual carriers:

$$\mathbf{J}(i,j,k) = \frac{q}{\Delta x \Delta y \Delta z} \left( \sum_{n=1}^{N^h(i,j,k)} S^h(i,j,k,n) \mathbf{V}^h(i,j,k,n) - \sum_{n=1}^{N^e(i,j,k)} S^e(i,j,k,n) \mathbf{V}^e(i,j,k,n) \right) \quad (1)$$

where  $S^h, e$  and  $\mathbf{V}^h, e$  are the super charges and velocities associated with the holes and electrons within the  $(i,j,k)$ th cell,  $N^e$  and  $N^h$  are the number of holes and electrons in the  $(i,j,k)$ th cell, and  $\Delta x$ ,  $\Delta y$ , and  $\Delta z$  represent the mesh spacings in the three directions. This three dimensional current density, which is effectively located at the center of the cell, is again converted through proper transforms in order to suitably interact with the electromagnetic fields [4-5].

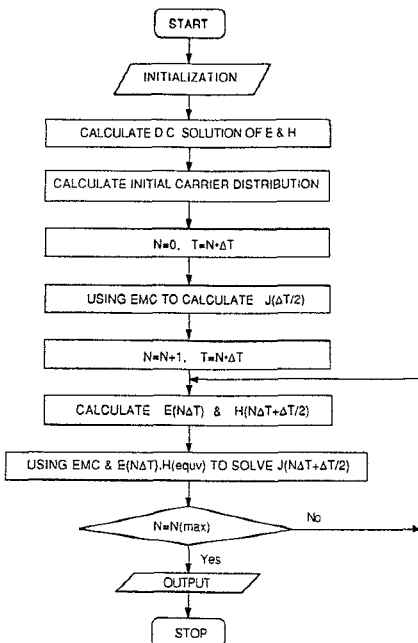


Fig. 1 The flow-chart.

The flow chart outlining the steps used in coupling the two models can be seen in Fig. 1.

## RESULTS

This technique was used to simulate the photoconductive switch, shown in Fig. 2. This structure represents one of the fastest switches available, with rise times in the subpicosecond range.

The actual device is made up of coupled microstrip lines on semi-insulating GaAs substrate. A thin plate of LiTaO<sub>3</sub>, with a high reflectivity coating on its lower surface, is placed on the device. A small window is etched into the coating to allow for transmission of the excitation beam onto the photoconductive gap. Fringing fields from the substrate extend into the electro-optic superstrate, and are detected and measured as a change in the polarization of the probe beam [3].

In our simulation, the thickness of the dielectric material,  $Dx$ , is  $4.5\mu\text{m}$ . The width of each strip,  $W_s$ , is  $2\mu\text{m}$  and the separation between them,  $W_g$ , is  $4\mu\text{m}$ . One of the strips is grounded at both ends, while the other has a gap,  $L_g$ , of  $5\mu\text{m}$  with one end grounded and the other end connected to an 8 volt DC source. The overall structure has dimensions  $L_x = 7\mu\text{m}$ ,  $L_y = 14\mu\text{m}$ , and  $L_z = 120\mu\text{m}$ . The entire space is

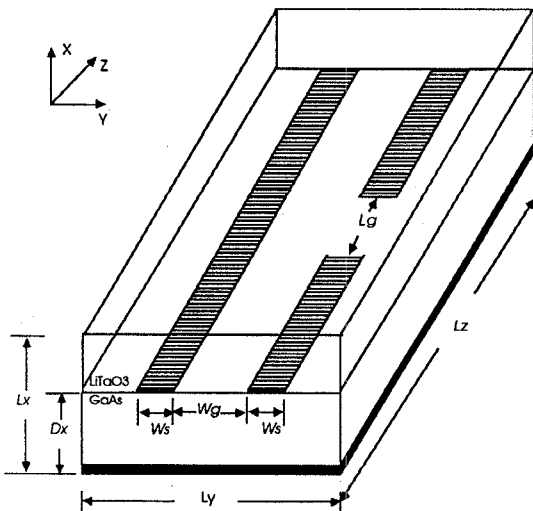


Fig. 2 Dimensions of device under simulation.

discretized using a three dimensional mesh with a uniform grid spacing of  $0.5\mu\text{m}$ . A laser pulse of energy  $1.55\text{eV}$  and  $30\text{fs}$  (FWHM) duration is applied to the gap, generating a carrier concentration of  $3 \times 10^{16} \text{ cm}^{-3}$ .

The electron velocity obtained from our first simulation is shown in Fig. 3. This simulation has the finite difference mesh bounded by electric walls, which has the effect of inclosing the entire structure in a metal box. In the electron velocity plot we see very little velocity overshoot. This is because the fields from the gap propagate away and strike the metal boundary. In doing so, they experience a  $180^\circ$  phase shift and propagate back into the gap and degrade the field, thereby giving the impression that the field in the gap is smaller than it actually is. Next, absorbing boundary conditions are added. The electron velocity obtained from this simulation is shown in Fig. 4. This simulation exhibited an increase in the velocity. Again this can be explained by the removal of the reflected fields that degraded the fields in the gap. Finally, Fig. 5 shows the results from a simulation that included absorbing boundary conditions and an electro-optic superstrat. As can be seen, the velocity overshoot has increased. This can be explained by considering reflections at the GaAs/LiTaO<sub>3</sub> interface. Now that the crystal has been added electromagnetic energy flows into the superstrat, increasing the field in the gap. The results presented in this figure are very similar to the experimental ones [3].

Now we look at several plots of the electric field just below the GaAs/LiTaO<sub>3</sub> interface. Shown in Fig.'s 6 and 7 are the DC x and z components of the electric field. Next, Fig.'s 8 and 9 show the AC x and z components of the electric field at  $t = 1 \text{ ps}$ . The AC plots were obtained by subtracting the proper DC field from the total field at 1 picosecond. These plots show that the electric field in the gap is non-uniform. This can be understood by realizing that the applied electric field pushes the electrons and holes in opposite directions, thus forming a quasi-dipole. This quasi-dipole increases the electric field near the electrodes, and reduces it in the center [4].

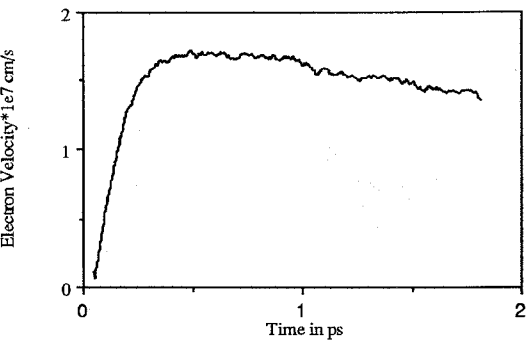


Fig. 3 Electron velocity from simulation in which the entire material was enclosed in a metal box.

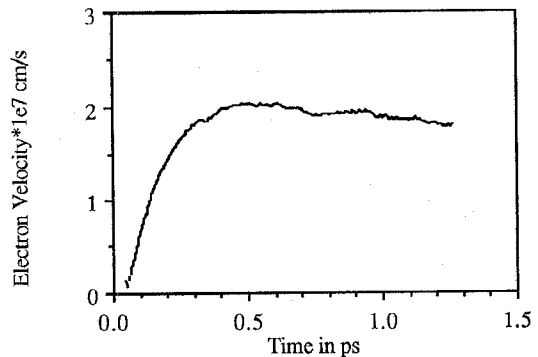


Fig. 4 Electron velocity after absorbing boundary conditions were added to the simulation.

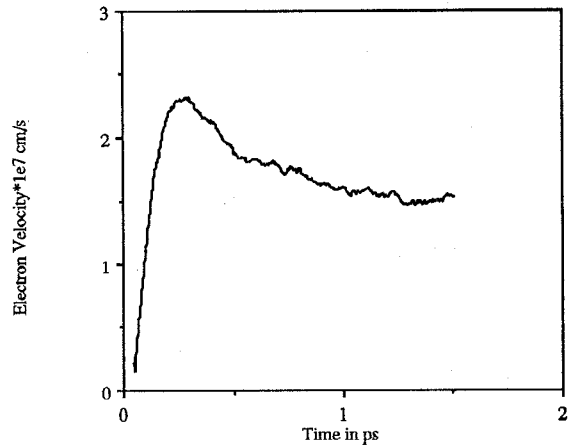


Fig. 5 Electron velocity from a simulation which included absorbing boundary conditions and an electro-optic superstrat.

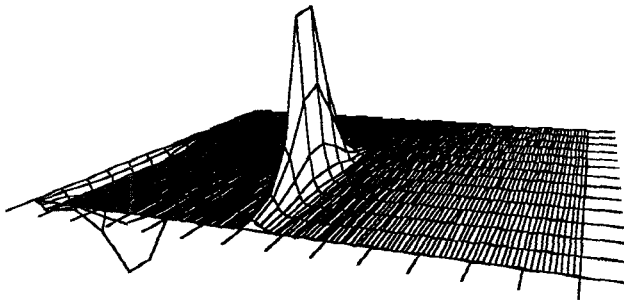


Fig. 6 Z component of the DC electric field below the GaAs/LiTaO<sub>3</sub> interface.

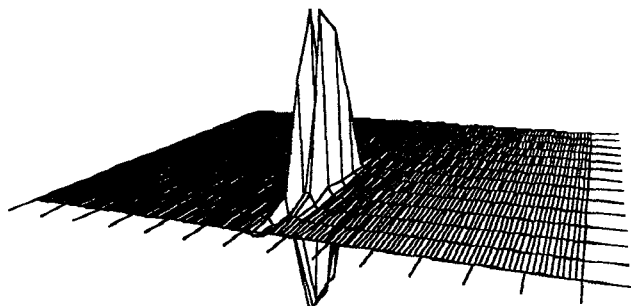


Fig. 8 Z component of the AC electric field at 1 picosecond below the GaAs/LiTaO<sub>3</sub> interface.

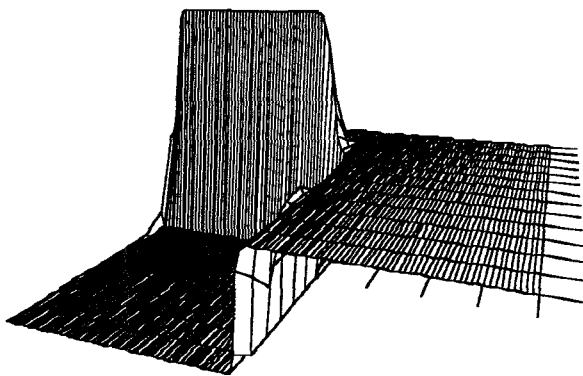


Fig. 7 X component of the DC electric field below the GaAs/LiTaO<sub>3</sub> interface.

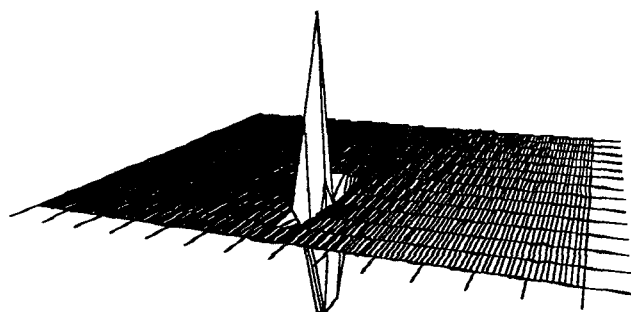


Fig. 9 X component of the AC electric field at 1 picosecond below the GaAs/LiTaO<sub>3</sub> interface.

## CONCLUSION

We presented an accurate model for studying transients in semiconductor devices and optical switches. This approach couples a direct solution of Maxwell's Equations with an Ensemble Monte-Carlo model. This model is capable of simulating very high frequency devices and switches on the subpicosecond scale. Optical interaction with semiconductor devices can also be modeled.

## ACKNOWLEDGEMENTS

The authors would like to thank G. Mourou, K. Meyer and D. Ferry for many helpful discussions, and M. Walker for proof reading the manuscript.

This work was supported by the RIA program at Arizona State University, the Air Force Office of Scientific Research, and the National Science Foundation.

## REFERENCES

[1] X. Zhang, and K.K. Mei, "Time-Domain Finite Difference Approach to the Calculation of the Frequency-Dependent Characteristics of Microstrip Discontinuities," *IEEE Trans. Microwave Theory Tech.*, Vol. 36, no.12, pp. 1775-1787:1988.

[2] G. Mur, "Absorbing Boundary Conditions for the Finite Difference Approximation of the Time-Domain Electromagnetic Field Equations," *IEEE Trans. Electromagn. Compat.*, Vol. 23, no.4, pp. 377-382:Nov. 1981.

[3] S.N. Chamoun, R. Joshi, E.N. Arnold, R.O. Grondin, K.E. Meyer, M. Pessot, and G.A. Mourou, "Theoretical and Experimental Investigations of Subpicosecond Photoconductivity," *J. Applied Physics.*, Vol. 66, No. 1, pp. 2346-2356:July 1989.

[4] Y. Lu, R.P. Joshi, S. El-Ghazaly, and R.O. Grondin, "Time Domain Finite Difference and EMC Study of Hot Carrier Transport in GaAs on a Picosecond Scale," *Solid State Electronics*, Vol. 32, no. 12, pp.1297-1301:1989.

[5] R.O. Grondin, R. Joshi, K. Connolly, and S. El-Ghazaly, "Physical Modeling of Ultrafast Electrical Waveform Generation and Characterization," *1990 Symp. Advances in Semiconductors and Superconductors: Physics Toward Device Applications*, San Diego, California, March 1990.